CANCER GENOMICS & PROTEOMICS *11*: 115-126 (2014)

Crucial and Novel Cancer Drivers in a Mouse Model of Triple-negative Breast Cancer

JACOB P. S. JOHNSON[1*], PRASHANT KUMAR[2], MIROSLAV KOULNIS[3], MILAN PATEL[4] and KARL SIMIN[1]

[1]*Department of Cancer Biology, University of Massachusetts Medical School, Worcester, MA, U.S.A.;*
[2]*Institute of Molecular and Cell Biology, A*STAR, Singapore;*
[3]*National Institute of Arthritis and Musculoskeletal and Skin Diseases, National Institutes of Health, Bethesda, MD, U.S.A.;*
[4]*Wright Center for Graduate Medical Education, Scranton, PA, U.S.A.*

Abstract. *Background: We previously developed a mouse model of breast cancer that mimics human triple-negative breast cancer (TNBC) by inactivating the Retinoblastoma (Rb), Transformation related protein 53 (p53), and Breast cancer 1 (Brca1) pathways in the mammary gland. Despite inactivation of all three tumor suppressors throughout the epithelium, low tumor multiplicity indicated that malignant carcinoma progression requires additional oncogenic stimuli. Materials and Methods: In order to identify collaborating genetic events, we performed integrated analysis of 18 tumors (eight tumors with inactivation of pRbf/Brca1/p53 and ten tumors with inactivation of pRbf/p53) using comparative genomic hybridization and global gene expression. We then conducted flow cytometric analysis, immunostaining, tumorsphere, and cell viability assays. Results: Copy number aberrations were correlated with the transcript levels of 7.55% of genes spanned by the altered genomic regions. Recurrent genomic losses spanning large regions of chromosomes 4 and 10 included several cell death genes. Among the amplified genes were well-known drivers of tumorigenesis including Wingless-related MMTV integration site 2 (Wnt2), as well as potentially novel driver mutations including the Late cornified envelope (LCE) gene family. These tumors have a stem/luminal progenitor phenotype and active β-catenin signaling. Tumorsphere formation and cell survival are suppressed by Wnt pathway inhibitors. Conclusion: Our novel mouse model mimics human TNBC and provides a platform to triage the pathways that underlie malignant tumor progression.*

Breast cancer remains the most prevalent form of cancer among women, accounting for over 39,000 deaths in the USA in 2012 (1). Systematic genomic surveys of tumors continue to expand the list of genes that are mutated, lost, or amplified in cancer. An important but complex task is defining the biological and clinical relevance of these genetic alterations, since a major goal of personalized medicine is to tailor treatments to the specific molecular changes in an individual's tumor. However, our ability to identify mutations has far outpaced our understanding of the relative impact of these events. Genetically engineered mouse models provide an experimental platform to address this challenge, since one route to prioritizing these efforts is identifying paralogous mutations in engineered mice that closely mimic the salient features of human cancer (2).

We previously generated a novel mouse model of triple negative breast cancer (TNBC) by inactivating the *Retinoblastoma* (*Rb*), *Transformation related protein 53* (*p53*), and *Breast cancer 1* (*Brca1*) pathways in mammary epithelium (3) because these tumor suppressors are frequently perturbed in the most aggressive forms of the disease. The mice developed highly aggressive, metastatic adenocarcinomas that exhibited global gene expression signatures similar to human basal-like and claudin-low subtypes of breast cancer. Basal-like and claudin-low breast cancers are two TNBC molecular subtypes that are defined by their transcriptional profiles (4). The biological relevancy of the mouse models is underscored by the discovery of the claudin-low subtype (5), which was originally defined in a cross-species genomic comparison between human and mouse breast cancers.

Here, we report our integrative comparative genomic hybridization (CGH) and gene expression analysis of tumors

*Present address: Columbia University, New York, NY, USA.

Correspondence to: Karl Simin, Ph.D., Department of Cancer Biology, University of Massachusetts Medical School, Worcester, MA 01605, U.S.A. Tel: +1 5088563959, Fax: +1 5088561310, e-mail: karl.simin@umassmed.edu

Key Words: Breast cancer, CGH, integrative analysis, tumor suppressor, oncogene, mouse model, triple-negative, *Wnt, Myc, Arid, Mapk, LCE.*

derived from our novel mouse model. Our motivation to perform a joint analysis of gene expression and copy number data derives from the expected correlation between genomic copy number and gene expression levels, as genomic loss should reduce expression levels, while increased copy number should lead to greater gene expression levels. We postulate that genes that meet these criteria are more likely drivers of tumorigenesis than merely bystander mutations. Support for this hypothesis comes from our identification of well-known oncogenic mutations.

To identify potential collaborating genetic events, we analyzed the genomic data we previously generated (3) from 18 mouse mammary tumors (eight tumors with inactivation of *pRb$_f$/Brca1/p53* and ten tumors with inactivation of *pRb$_f$/p53*) using comparative genomic hybridization and global gene expression. From these bioinformatics analyses the Wnt/β-catenin/TCF signaling axis emerged as a candidate pathway that shaped the biology of these tumors. Therefore, we initiated an experimental validation of the role of Wnt/β-catenin/TCF signaling. We conducted flow cytometric analysis, immunostaining, tumor-sphere, and cell viability assays to examine the impact of Wnt/β-catenin/TCF signaling on the tumor biology. Novel genes identified through this approach may provide further insights into the mechanisms that underlie breast cancer evolution and potentially point to new therapeutic avenues.

Materials and Methods

Ethics statement. This study was executed in strict adherence to the recommendations in the Guiding Principles in the Care and Use of Animals approved by the Council of the American Physiological Society. The mice were always treated humanely under the guidance of an expert in this field.

TBP Mouse tumor samples. Tumor specimens for the validation studies were obtained from *TgMFT$_{121}$*; *TgWAP-Cre*; *Brca1$^{f/f}$*, *p53$^{f/f}$* mice that are maintained in our mouse colony and genotyped by PCR using previously published protocols (3). Tumorigenesis is initiated in female mice by pregnancy-induced *WAP-Cre* transgene expression.

Bacterial artificial chromosome (BAC) annotations. We revised the mapping annotations of the University of California, San Francisco mouse genomic array (GEO GPL9906). Firstly, we determined the ends of the BACs spotted on the array by querying the clone names against University of California Santa Cruz (http://genome.ucsc.edu/) and National Center for Biotechnology Information databases (Build 37). Of the clones with defined BAC endpoints, most had been fully sequenced. For the 383 clones (17%) without known BAC end sequences, we approximated their length as equal to the average length of the 1,833 (83%) clones with definitive BAC end points (212 kb).

Integrative CGH and gene expression analysis. Using algorithms implemented in BRB-CGH Tools (Richard Simon, Biometric Research Branch-National Institutes of Health), we analyzed CGH (GEO GSE40925) and mRNA expression data (GEO GSE34479) of 18 tumors that we previously reported (3). Copy number data were segmented with the improved circular binary segmentation algorithm (6) and we generated a frequency plot with a threshold based on the segmentation $\log_2$ ratios. The threshold $\log_2$ ratio for amplifications and homozygous deletions was ±0.2, and the gain and loss threshold was ±0.1. We used the Genome Identification of Significant Targets in Cancer (GISTIC) to identify regions with frequent DNA copy number gains and losses (7). For the integrated analysis of copy number aberration (CNA) and expression data, we used the Pearson's correlation method with a cut-off p-value of 0.05. We used BRB ArrayTools to generate a heat map of β-catenin-modulated genes (8).

Pathway analysis. We used the FatiGO tool implemented in the Babelomics 4.3.0 integrative platform (babelomics.bioinfo.cipf.es) with parameters set for the Fisher's exact two-tailed test to determine the enriched Kyoto Encyclopedia of Genes and Genomes (KEGG) pathways among the differentially expressed genes determined by BRB-CGH Tools. We also used the BRB-CGH Tools to find significant BioCarta pathways enriched for gains and losses with a threshold *p*-value of 0.05.

Flow cytometric analysis. Flow cytometric analysis was carried out using FlowJo (Tree Star, Inc., Ashland, OR, USA) and the following antibodies from BioLegend, San Diego, CA, USA unless otherwise noted: 0.25 μg/ml CD49f-APC (GoH3), 5 μg/ml CD24-Pacific Blue (M1/69), CD61-PE (2C9.G2), and lineage (Lin) markers Ter-119-PE, CD31-PE (MEC13.3), and CD45R-PE (RA3-6B2). Cells were suspended in the hemochromatosis gene at 5×10^6/ml, and incubated with the indicated antibodies as well as 7-aminoactinomycin D (7-AAD; BD Biosciences, San Jose, CA, USA) for 45 min on ice. Cells were washed thrice in 0.5% bovine serum albumin in phosphate buffered saline, and kept on ice. Live single cells (fixed FSC-A/FSC-W ratio; 7-AAD negative) were gated for analysis. Enrichment for mammary epithelial cells and their flow cytometry was performed using APC-CD49f and Pacific Blue-CD24.

Immunostaining. Immunohistochemical analysis was carried on formalin-fixed paraffin sections. Antigen retrieval was achieved by boiling the slides in citrate buffer pH 6.0 (Zymed, South San Francisco, CA, USA) for 15 min. We used antibodies directed against β-catenin (E-5, SC-7963; Santa Cruz Biotechnology, Dallas, TX, USA) and keratin 6 (PRB-169P; Covance, Princeton, NJ, USA). Detection for all antibodies was performed using the Vector ABC Elite kit (Vector Laboratories, Burlingame, CA, USA). All immunofluorescence reactions were carried out using AlexaFlour-conjugated secondary antibodies (AlexaFluor 488 and 594; Molecular Probes, Thermo Fisher Scientific Inc., Waltham, MA, USA). Slides were counterstained with 4',6-diamidino-2-phenylindole (DAPI) and mounted using Hardset Mounting Media (Vector Laboratories, Burlingame, CA, USA).

Tumorsphere assay. Primary mammary tumors were mechanically minced and digested as previously described (9, 10). Briefly, tumors were sequentially digested at 37˚C in 300U/ml collagenase (Gibco, Thermo Fisher Scientific Inc., Waltham, MA, USA) plus 100 U/ml hyaluronidase (Sigma-Aldrich, St. Louis, MO, USA) for 2 hours, 0.25% trypsin (Gibco) for 2 minutes, and 5 mg/ml Dispase II

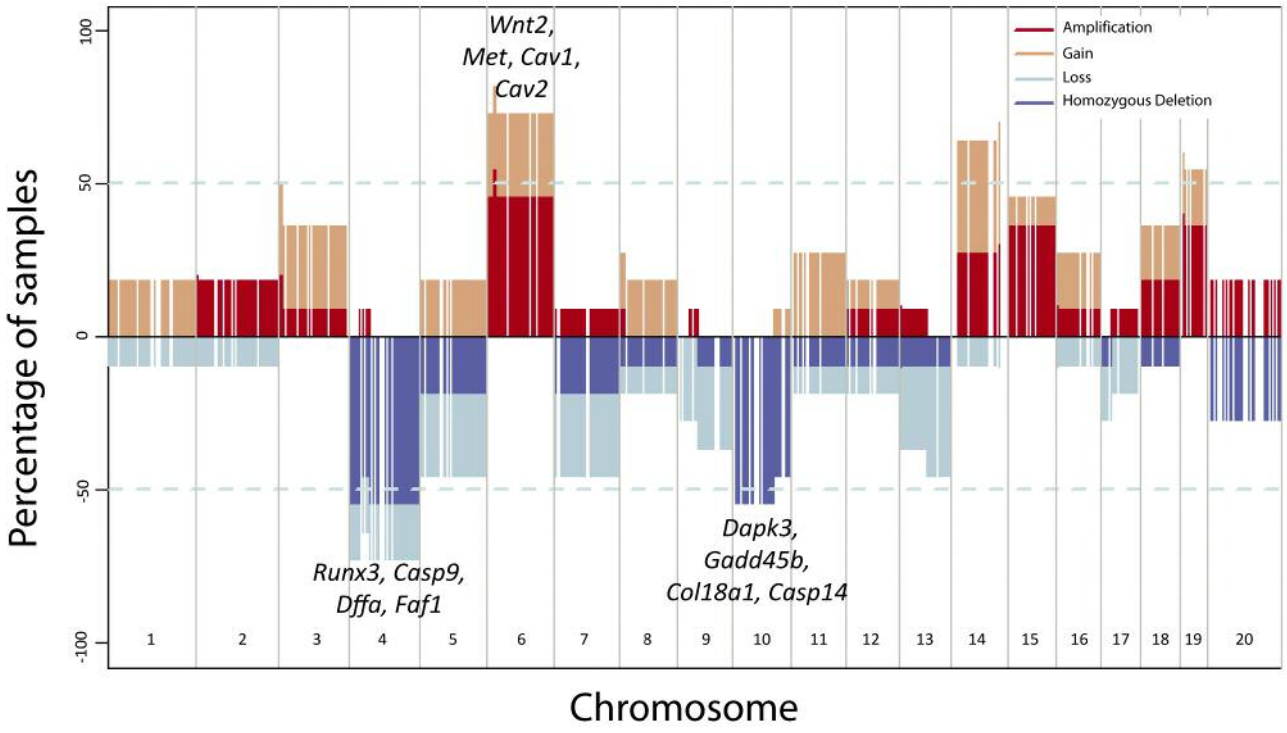

Figure 1. *Summary of frequent copy number aberrations. On each of twenty chromosomes, red lines above indicate statistically significant (p<0.05) amplifications and gains, and blue lines below indicate losses and homozygous deletions. Potential key oncogenes are labeled above chromosome 6 and potential key tumor suppressors are labeled below chromosomes 4 and 10.*

(Roche, Basel, Switzerland) plus 0.1 mg/ml DNaseI (Sigma) for 5 minutes. Cells were filtered through a 40 μm mesh. Cells were then plated in 3 ml of defined mammosphere media (11): Dulbecco's modified Eagle's medium:F12 medium (serum free) supplemented with 20 μl/ml B27 (Invitrogen, Thermo Fisher Scientific Inc., Waltham, MA, USA), 20 ng/ml epidermal growth factor, 20 ng/ml basic fibroblast growth factor, and 0.5% methylcellulose per well of a 6-well ultra-low attachment plate (Corning Life Sciences, Tewksbury, MA, USA), at a density of 10^4 cells/ml. Fresh medium (500 μl) was added every third day. Treated cells were incubated with 1 μM of the tankyrase inhibitor XAV939 (Sigma). Mammospheres were counted on day 10.

Cell viability determination. Approximately 10^5 cells were transfected with pGipz-dnTCF4 (a kind gift from J. Mao at University of Massachusetts Medical School) or empty vector, then incubated for four days in medium supplemented with 2 μg/ml puromycin. Subsequently, 3000 trypsin-dissociated cells were plated in quadruplicate and assayed by MTT assay after five days. The mean proportion of viable cells and their standard deviation were reported.

Results

CNAs and associated pathways in tumors from a mouse model of TNBC. Significant recurrent deletions occurred on chromosomes 4 and 10 (>50% of samples). These two genomic regions harbor many known tumor suppressors, including *Caspase 14* (*Casp14*), *Casp9*, *Growth arrest and DNA-damage-inducible 45 beta* (*Gadd45b*), and *Runt related transcription factor 3* (*Runx3*) (Figure 1, Table I). Many of these genes and their associated pathways carry out crucial cellular functions, such as regulation of autophagy (p=0.00269) for degradation of cellular components, p53 signaling (p=0.00846) for apoptosis, and Janus kinase-Signal Transducer and Activator of Transcription (JAK-STAT) signaling (p=0.000984) for response to extracellular chemical signals. Other recurrent losses localized to chromosomes 5, 7 and 13 (Figure 1). Losses and deletions were more prominent than amplifications and gains, which is a signature feature of this highly penetrant mouse model. In contrast to the large domains of chromosomes 4 and 10 that were lost, encompassing 2,154 genes, only a small length of chromosome 6 spanning only nine genes was amplified.

On this region of chromosome 6 (6qA2), the oncogenes *Wnt2, Met proto-oncogene* (*Met*), *Caveolin 1* (*Cav1*), and *Cav2* were amplified (Table I). Focal adhesion was the most enriched pathway (p=0.0104) associated with these genes. This amplified region is paralogous to human chromosome 7q31.1-31.3, which shows high level amplifications in

Table I. *The 50 most significant genes whose expression correlated with CNA.*

	Genes symbol	Location	Number of observations	Correlation coefficient	*p*-Value	False discovery rate (FDR)
1	*A430005*					
	L14Rik	Chr3q	11	0.9175	<0.0001	0.1112
2	*Commd4*	Chr4q	11	0.9599	<0.0001	0.0184
3	*Nubp2*	Chr9q	11	0.9249	<0.0001	0.1112
4	*Elf2*	Chr17q	11	0.9249	<0.0001	0.1112
5	*Timm8b*	Chr9q	11	0.9249	0.0002	0.4111
6	*St3gal5*	Chr6q	11	0.9249	0.0002	0.4111
7	*Vmn2r30*	Chr7q	11	0.9249	0.0002	0.4111
8	*Ssr1*	Chr13q	11	0.9249	0.0003	0.4111
9	*Ttc4*	Chr4q	11	0.9249	0.0003	0.4111
10	*Zfp954*	Chr7q	11	0.9249	0.0003	0.4111
11	*Ms4a4b*	Chr19q	9	0.9249	0.0003	0.4111
12	*Bicd2*	Chr13q	10	0.9249	0.0004	0.4111
13	*Slc25a11*	Chr11q	11	0.9249	0.0005	0.4111
14	*Fam177a*	Chr12q	11	0.9249	0.0005	0.4111
15	*Lce1c*	Chr3q	11	0.9249	0.0005	0.4111
16	*Fdx1*	Chr9q	11	0.9249	0.0005	0.4111
17	*Spc24*	Chr9q	11	0.9249	0.0006	0.4111
18	*Gpsm3*	Chr17q	11	0.9249	0.0007	0.4111
19	*Lce1e*	Chr3q	11	0.9249	0.0007	0.4111
20	*Lce1i*	Chr3q	11	0.9249	0.0007	0.4111
21	*Lce1d*	Chr3q	11	0.9249	0.0007	0.4111
22	*Ripk1*	Chr13q	9	0.9249	0.0008	0.4111
23	*Twf2*	Chr9q	11	0.9249	0.0008	0.4111
24	*Ift122*	Chr6q	11	0.9249	0.0009	0.4111
25	*Ifngr1*	Chr10q	11	0.9249	0.001	0.4111
26	*Cwf19l1*	Chr19q	11	0.9249	0.001	0.4111
27	*Msi1*	Chr5q	11	0.9249	0.001	0.4111
28	*Hist1h1t*	Chr13q	11	0.9249	0.001	0.4111
29	*C130079*					
	G13Rik	Chr3q	6	0.9249	0.001	0.4111
30	*Nphs1*	Chr7q	7	0.9249	0.001	0.4111
31	*Lce1b*	Chr3q	10	0.9249	0.001	0.4111
32	*Cs*	Chr10q	11	0.9249	0.0011	0.4111
33	*Nfil3*	Chr13q	11	0.9249	0.0011	0.4111
34	*Traf3*	Chr12q	11	0.9249	0.0012	0.4111
35	*Ipp*	Chr4q	11	0.9249	0.0012	0.4111
36	*Cmc1*	Chr9q	11	0.9249	0.0012	0.4111
37	*Arid3a*	Chr10q	11	0.9249	0.0012	0.4111
38	*Rg9mtd2*	Chr3q	11	0.9249	0.0012	0.4111
39	*Apitd1*	Chr4q	11	0.9249	0.0012	0.4111
40	*Sgk2*	Chr2q	10	0.9249	0.0014	0.4127
41	*B3galt2*	Chr1q	5	0.9249	0.0014	0.4127
42	*D630045*					
	J12Rik	Chr6q	11	0.9249	0.0014	0.4127
43	*Prrg2*	Chr7q	11	0.9249	0.0014	0.4127
44	*Frmd4b*	Chr6q	10	0.9249	0.0014	0.4127
45	*Rpsa*	Chr9q	11	0.9249	0.0015	0.4284
46	*Gtpbp4*	Chr13q	10	0.9249	0.0016	0.4284
47	*Ubiad1*	Chr4q	11	0.9249	0.0016	0.4284
48	*Dedd*	Chr1q	11	0.9249	0.0016	0.4284
49	*Cpa3*	Chr3q	11	0.9249	0.0017	0.438
50	*Fig4*	Chr10q	11	0.9249	0.0019	0.4528

invasive serous carcinomas (12). Another potential amplification was on chromosome 15 which harbors the well-described proto-oncogenes *Wnt1* and *Myc* (Figure 1).

Integrated analysis. Despite the proven role of *Brca1* in maintaining genomic integrity, we previously reported that there is no significant difference between the average number of CNAs in tumors where all three tumor-suppressor pathways are perturbed (TBP tumors) *versus* tumors where only *Rb* and *p53* are inactivated (TP tumors) (3). However, our integrated analysis here shows that there are significantly more genes in TBPs than in TPs whose expression correlated with CNAs ($p<0.0001$, Chi-square with Yates correction, two-tailed). Only 5.36% of TP genes were correlated, while 7.96% of TBP genes were correlated.

We identified the top 50 statistically significant genes whose expressions were correlated with CNAs (Table I). The Toll-like receptor signaling pathway ($p=0.00008888$) and glyoxylate and dicarboxylate metabolism ($p=0.0004844$) are prominently enriched pathways among these genes. The Toll-like receptor 4 is overexpressed in numerous types of human cancer, including in cervical cancer, where it promotes immunosuppressive cytokine production (13, 14), and in prostate cancer, where it causes chemoresistance to docetaxel (15). The differential expression of glyoxylate and dicarboxylate metabolism has been implicated as a cause in acute myeloid leukemia (16) and in lung adenocarcinomas due to loss of cell differentiation (17). Gene families that had numerous members represented among all 972 correlated genes identified by integrative analysis include the *B3* and *B4 galt, BC, Cdc, Cd, Fam, Mapk, Ppp, Rab, Slc, Tmem, Tnf,* and *Zfp* families. Ten percent of the top 50 genes encode the late cornified envelope proteins (*Lce1b, Lce1c, Lce1d, Lce1e, Lce1i*), which are normally associated with the keratinocyte terminal-differentiation pathway and cornification of skin, which is a type of cell death distinct from apoptosis (18).

We observed a strong overlap between the top 23 KEGG pathways enriched among genes identified by integrative analysis in our model, the top 23 pathways identified by Shah *et al*. in human TNBC (19), and the top 23 pathways found by Ellis *et al*. in human estrogen-receptor-positive breast cancer (20) (Figure 2A). A word cloud (Figure 2B) highlights the genes most often shared among these oncogenic pathways. Prominent genes include *Arid3a*, an *E2F*-related gene, and *Map2k2, Pik3r1, Hoxa5, Akt1*, and *Nfkbia*. Analysis of BioCarta pathways identified additional targets of cancer therapeutics. The enriched control of the cell cycle and breast tumor growth by the estrogen-responsive finger protein (efp) may account in part for our tumor model's similarity with estrogen-receptor-positive breast cancer characterized by Ellis *et al*. (20). Given the role of numerous cyclin-dependent kinases in this pathway and

A

Overlapping enriched pathways

ER-positive BrCa		TBP mouse model		Human TNBC	
Pathway	***p*-Value**	**Pathway**	***p*-Value**	**Pathway**	***p*-Value**
Melanoma	1.37E-42	Neurotrophin signaling pathway	4.38E-03	Pathways in cancer	0
Non-small cell lung cancer	5.33E-36	Selenoamino acid metabolism	4.40E-03	Endometrial cancer	0
Endometrial cancer	1.50E-35	N-Glycan biosynthesis	5.27E-03	Melanoma	0
Chronic myeloid leukemia	2.32E-35	Cell cycle	6.46E-03	A6b1 and A6b4 Integrin signaling	0
Glioma	8.69E-35	Pathways in cancer	2.19E-02	Integrin signalling pathway	0
Prostate cancer	9.04E-34	Toll-like receptor signaling pathway	1.04E-02	Small cell lung cancer	0
Pancreatic cancer	1.48E-30	Oxidative phosphorylation	1.04E-02	Non-small cell lung cancer	0
Colorectal cancer	3.16E-30	Prostate cancer	1.04E-02	Prostate cancer	0
Neurotrophin signaling pathway	1.67E-26	Adipocytokine signaling pathway	1.75E-02	Glioma	0
Apoptosis	1.65E-24	Chronic myeloid leukemia	9.32E-03	Focal adhesion	0
Small cell lung cancer	3.01E-24	B-cell receptor signaling pathway	2.21E-02	Pancreatic cancer	0
Acute myeloid leukemia	8.81E-23	Glioma	2.21E-02	Bladder cancer	0
Pathways in cancer	2.89E-22	Cyanoamino acid metabolism	2.21E-02	mTOR signaling pathway	0
mTOR signaling pathway	3.68E-22	Primary bile acid biosynthesis	2.38E-02	Il-7 signal transduction	0
Renal cell carcinoma	9.28E-22	Renal cell carcinoma	3.06E-02	p53 pathway feedback loops 2	0
Hepatitis C	1.71E-21	Chondroitin sulfate biosynthesis	3.06E-02	Thyroid cancer	0
Fc epsilon RI signaling pathway	1.97E-19	Thyroid cancer	3.23E-02	Pten-reliant cell cycle arrest and PCD	0
ErbB signaling pathway	4.42E-19	Apoptosis	3.80E-02	Chronic myeloid leukemia	0
Aldosterone-regulated Na reabsorption	7.67E-19	Homologous recombination	4.19E-02	Renal cell carcinoma	0
Toll-like receptor signaling pathway	1.84E-18	Glycosphingolipid biosynthesis	4.19E-02	Growth hormone signaling pathway	0
Carbohydrate digestion and absorption	7.12E-18	Insulin signaling pathway	4.38E-02	Cardiovascular hypoxia and p53	0
B-cell receptor signaling pathway	1.52E-16	MAPK signaling pathway	4.62E-02	Cell cycle: G1/s check point	0
Bacterial invasion of epithelial cells	3.57E-16	T-cell receptor signaling pathway	4.95E-02	Wnt signaling pathway	0

All
TBP mouse model + ER-positive BrCa
TBP mouse model + human TNBC
ER-positive BrCa + human TNBC

B

Figure 2. *Significant pathways and their most involved genes. A: Overlap between the top 23 KEGG pathways identified by integrative analysis in our T_{121}/Brca1/p53 (TBP) mouse model and the top 23 pathways identified by Shah et al. in human triple-negative breast cancer (TNBC) (16) and by Ellis et al. in human estrogen-receptor-positive breast cancer (18). Red indicates overlap among all three types of cancer, yellow reveals intersection between estrogen receptor-positive breast cancer and our TNBC model, blue indicates overlap between human TNBC and our TNBC model, and green reveals intersection between ER-positive breast cancer and human TNBC. B: A word cloud depicting the genes that are involved in numerous highly enriched KEGG pathways. Word size correlates with the number of times a gene is present among the listed pathways.*

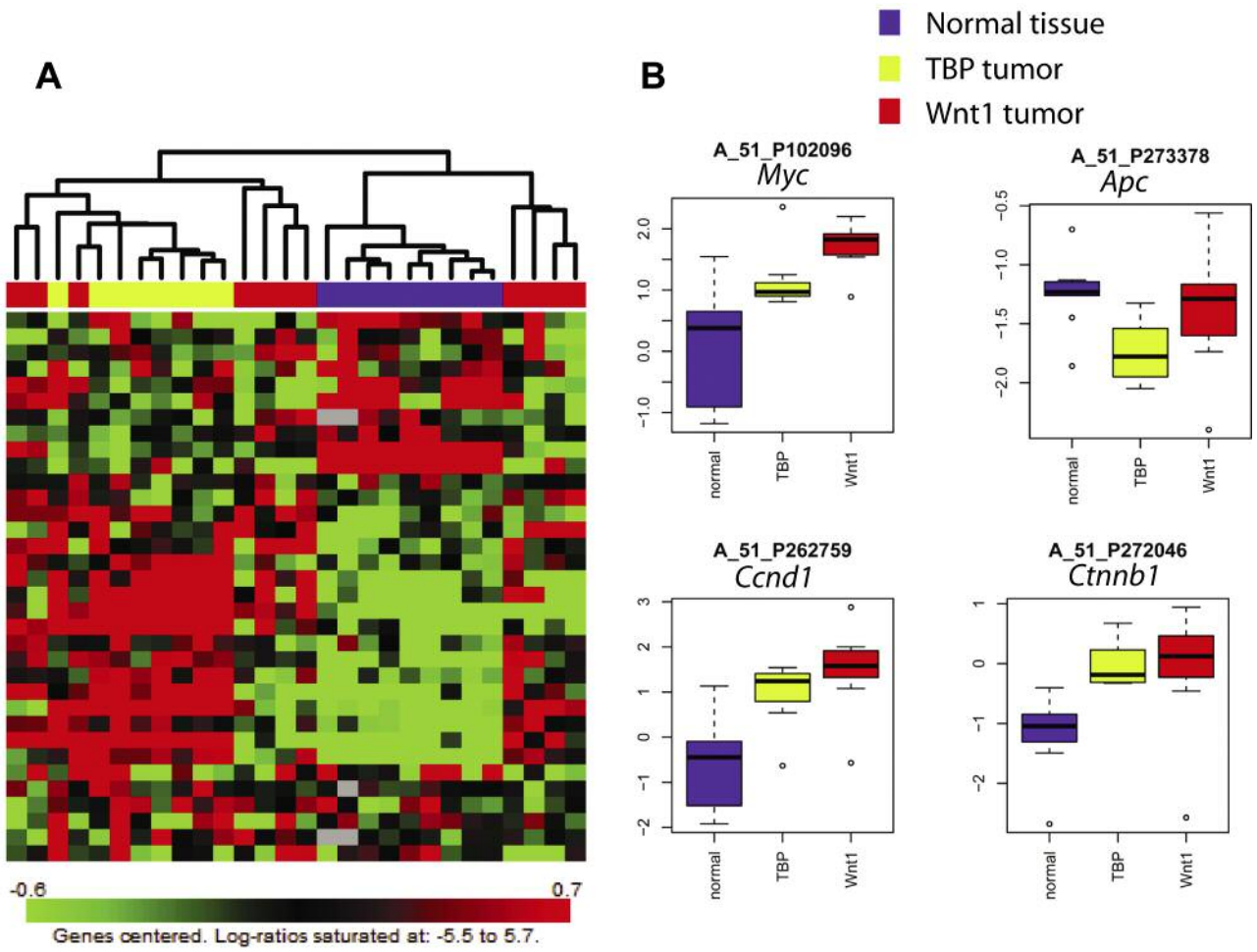

Figure 3. *T_{121}/Brca1/p53 (TBP) and mouse tumors derived from Wnt1 transgenic mice show correlated expression of β-catenin-target genes. A: Heat map of 34 up-regulated targets (8) in normal mammary tissue (blue), TBP (yellow), and Wnt1 (blue) mammary tumors assayed by genome-wide gene expression (3). B: Wnt pathway members β-catenin (Cctnb1), c-Myc, and cyclin D1 (Ccnd1) show elevated expression, while the negative regulator Adenomatosis polyposis coli (Apc) is reduced in TBP tumors.*

the numerous drugs that inhibit cyclin-dependent kinases (21), this pathway may be especially relevant to cancer therapeutics.

Numerous gained genes were correlated with the endoplasmic reticulum (ER)-associated degradation pathway (p=0.021). We hypothesize that these gained genes inhibit ER stress, causing a reduction of both apoptosis and tumor suppression. We also previously identified several highly enriched pathways in our mouse model by manual curation, including Parkinson's disease, maturity onset diabetes of the young, type II diabetes mellitus, Alzheimer's disease, and Huntington's disease, which are likely caused at least in part by ER stress (22-24). Therefore, further elucidating the role of ER stress in cancer will be critical in future studies.

The Wnt/β-catenin/TCF signaling pathway shapes TBP tumor biology. The Wnt pathway is a highly conserved pathway that mediates stem cell self-renewal and lineage fate determination in diverse tissues. This pathway has been targeted in TNBC in early phase clinical trials (25). We hypothesized that the Wnt/β-catenin/TCF signaling pathway plays a key role in shaping TBP tumor biology based on genome-wide gene expression, CNA, tumor histology, and preliminary studies of Wnt pathway inhibition. Both *Wnt1* and *Wnt2* loci were amplified in the present analysis, and our previous manual curation of CGH data showed a strong enrichment of the Wnt signaling pathway, including *Wnt2* and *Wnt8a* (p=3.13E-15). In addition, when we examined a signature (8)of β-catenin-regulated genes (Figure 3A), or specific Wnt pathway genes, including *Myc*, *Ccnd1*, and

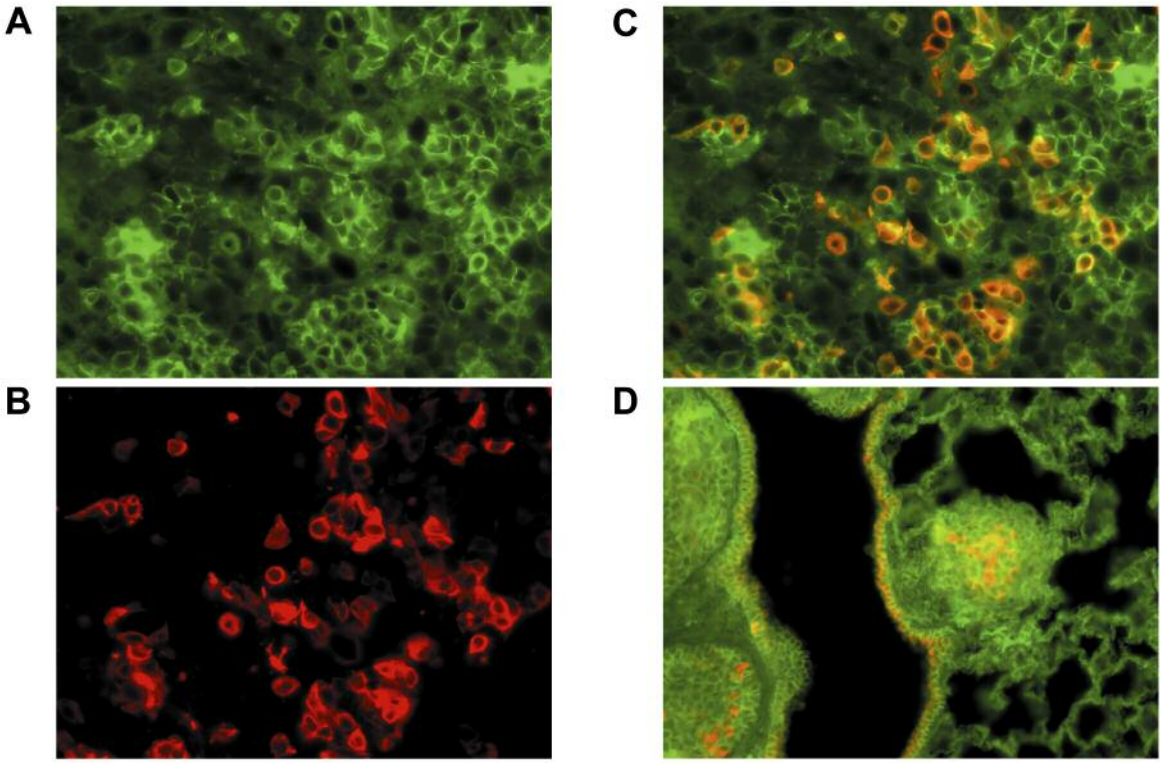

Figure 4. *β-Catenin signaling is active in TBP tumors/pulmonary metastases. β-Catenin (green) is cytoplasmic and nuclear in primary tumors (A and C, n=6) and in lung metastases (D, n=3). Keratin 6 (Krt6) (red, B, C, and D) is a biomarker of up-regulated β-catenin signaling.*

Ctnnb1 (Figure 3B), we observed similar patterns shared by TBP and *Wnt1*-induced mouse tumors (26). Notably, the integrative analysis of copy number and gene expression overlooked small, focal amplifications of *Wnt* genes that were identified by manual curation or the GISTIC algorithm. Nevertheless, numerous Wnt pathway regulators were identified by integrative analysis. For example, *Gsk3b* and *Tcf7* genes figured prominently among the enriched pathways identified by joint CGH and expression analysis (Figure 2B). Consistent with these gene expression data, both primary TBP tumors and lung metastases exhibited nuclear and cytoplasmic β-catenin immunostaining, supporting an active role for Wnt/β-catenin/TCF signaling in promoting tumors and metastasis (Figure 4A, C and D). Similarly, Keratin 6 (*Krt6*), a biomarker of elevated Wnt activity, was also abundant in primary TBP tumors and pulmonary metastases (Figure 4B-D).

TBP tumors exhibit a stem/luminal progenitor phenotype. Three observations prompted us to test the hypothesis that the TBP tumors are enriched for luminal stem and/or progenitor cells like human TNBC is. Our mouse model exhibits poorly differentiated tumor histology and gene expression patterns (3). Human basal-like *BRCA1*-mutated cancer also resembles luminal progenitor cells at the molecular level (27). Furthermore, Claudin-low tumors demonstrate enhanced self-renewal and tumorsphere-forming capacity, enrichment of tumor-initiating cells, and high expression of epithelial-mesenchymal transition (EMT)-inducing factors (28, 29).

Flow cytometric analysis was consistent with a model in which TBP tumors and tumor-derived cell lines have large populations of stem/progenitor cells. In mice, $Cd49f^{hi}$ $Cd24^{+}$ double-positive cells enrich for mammary stem cells that are capable of repopulating a fat pad cleared of epithelial cells (10, 30). This stem cell population is expanded in preneoplastic mammary glands and tumors of *MMTV-Wnt1* mice (30-33), thereby indicating a connection between the stem/luminal phenotype and Wnt signaling. We found that TBP tumors (n=3) had an abundance of $lin^{-}Cd49f^{hi}$ $Cd24^{+}$ cells (mean=48%, Figure 5A), which were positive or negative for the progenitor cell marker Cd61 (Figure 5B) (34). Cell lines established from TBP tumors (n=4) maintained high proportions of $Cd49f^{hi}Cd24^{+}$ cells, with a 52% greater amount than the immortalized, non-transformed, mouse mammary cell line NMuMG (ATCC CRL-1636).

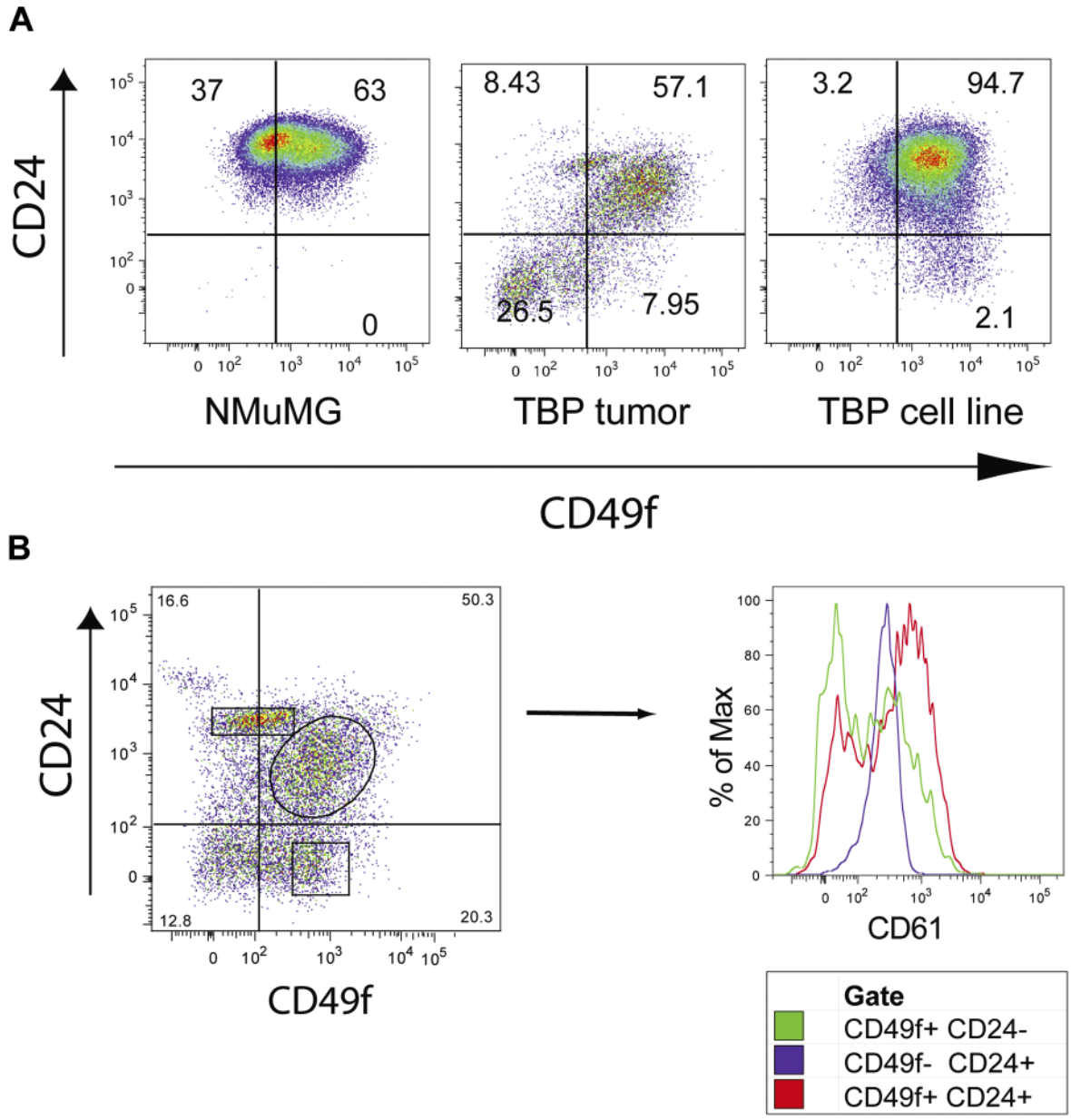

Figure 5. *Flow cytometric analysis reveals a stem/luminal progenitor phenotype. A: Cd49f^{hi}Cd24^{+} (cluster of differentiation) cells, which are reportedly enriched with tumor-initiating and luminal progenitor cells, are abundant in TBP tumors and cell lines compared to immortalized, non-transformed, normal murine mammary gland epithelial (NMuMG) cells. B: The Cd61 luminal progenitor marker is also more highly expressed in Cd49f^{hi}Cd24^{+} cells (circled) compared to the remaining cells.*

TBP tumor cells require the Wnt pathway for survival. We next tested the effect of Wnt pathway inhibition on tumorsphere formation. Five independent TBP tumor-derived cell lines formed tumorspheres when grown under low adhesion conditions (Figure 6A), a property shared by stem, progenitor, and tumor-initiating cells, presumably owing to enhanced anoikis resistance (35, 36). A single tested TBP cell line formed secondary tumors following serial transplantation into syngeneic (FVB) mammary fat pads (100%, n=3 mice), confirming the tumor-initiating and malignant capacity of this TBP cell line. We then examined the impact of Wnt pathway inhibition on TBP tumor cells *ex vivo*. Wnt pathway suppression by the tankyrase inhibitor XAV939 (37) reduced tumorsphere formation in five independent TBP cell lines

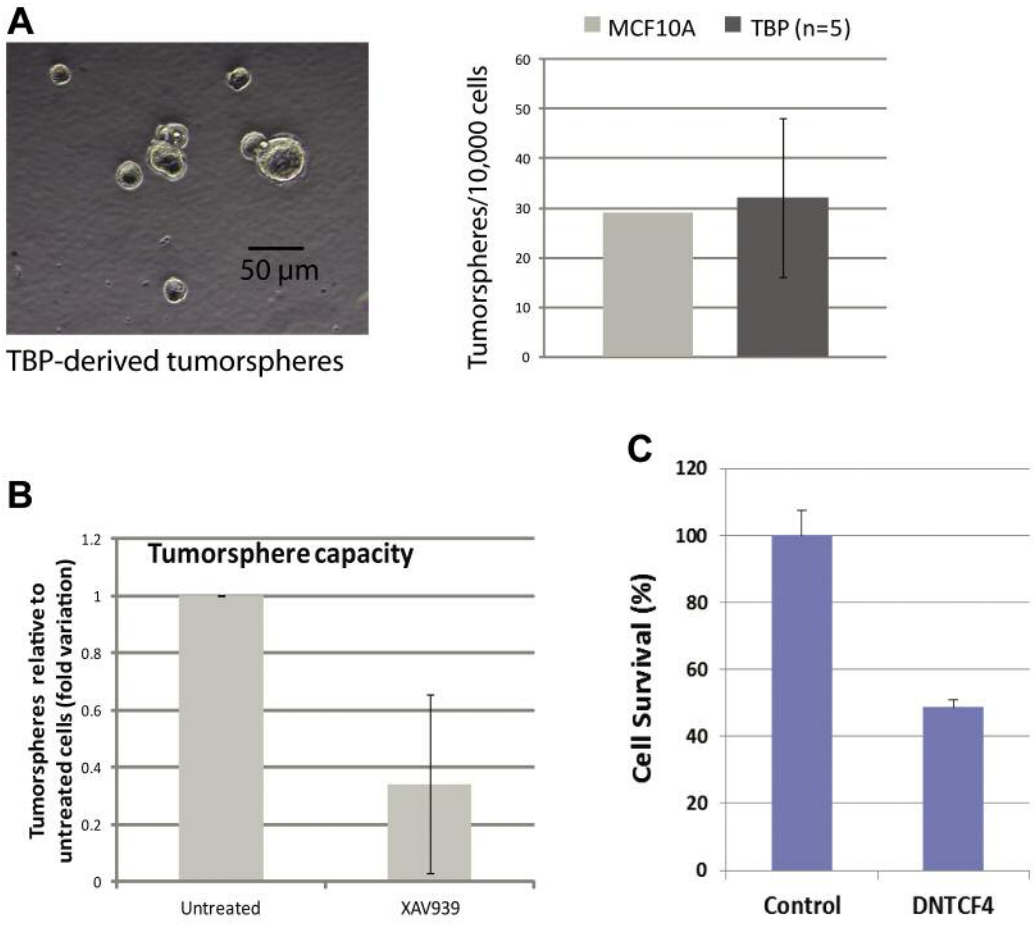

Figure 6. *Wnt pathway inhibition suppresses TBP tumorsphere growth and cell survival. Five independent tumor-derived cell lines showed variable capacity for tumorsphere growth in low adhesion culture conditions, with comparable levels, on average, to that of the human breast cancer cell line MCF10A (A). Treatment with tankyrase (XAV939) pathway inhibitor inhibited tumorsphere formation in five independent TBP cell lines (B; *p<0.008). Tumorsphere capacity is presented as the fold variation and SD of tumorsphere counts relative to that of untreated control cells. Dominant negative Transcription factor 4 (TCF4) cDNA transfection inhibited TBP cell survival (C; MTT assay).*

(Figure 6B, $p<0.008$, two-sided, paired *t*-test). Finally, we found that transfection of dominant-negative *TCF4* cDNA into TBP cells inhibited cell survival (Figure 6C). Future experiments will be important to establish whether Wnt pathway inhibition also reduces tumor initiation and cell survival capacity in vivo as predicted by these *in vitro* assays of stem/progenitor TBP cells.

Discussion

A significant drawback of using mouse models for genomic analyses of tumors is their tendency to yield recurrent, stereotypical CNAs, even across diverse tumor types (2). Although combined *Rb* and *p53* perturbations were sufficient for tumor formation after long latency (38, 39), by adding *Brca1* mutation we aimed to stimulate genomic instability in order to better mimic the mutational diversity observed among human tumors. As a result of triple pathway inactivation, we observed expression of 972 genes to be strongly correlated with CNAs. That these mutations were acquired after mere weeks of tumor growth attests to the remarkable ability of these tumors to rapidly acquire mutations that initiate and sustain tumorigenesis.

The strong correlation between enriched pathways in our model and those enriched in human data sets (Figure 2A) further supports the validity of these mice as a human cancer model. In human studies, *Myelocytomatosis oncogene* (*MYC*), *ERBB2*, and *KRAS* amplification, as well as *RB1* and *INTS6* loss, ranked among the most significant mutations (40-42). AKT, PTEN, and MAPK signaling pathways are among the most amplified pathways among enriched genes in human breast cancer (40, 43). Importantly, all of these

genes and pathways are represented among either the manually curated genes or those identified by the integrative analysis of the TBP tumor model (Tables I). Furthermore, Met, a gene up-regulated on a conserved amplicon of our model, has been shown to play a prominent role in inducing basal-like breast cancer (44, 45). Thus, these strong parallels in the molecular changes accrued in our mouse model and human TNBC underscore their particular relevance, especially to the basal-like and claudin-low molecular subtypes.

Neither manual curation nor the integrative analysis algorithm we employed was satisfactory on its own for detection of putative cancer drivers. Manual curation is time-consuming and prone to human error. In contrast, computer-based algorithms are rapid and automated, making these results far easier for others to replicate. However, the GISTIC parameters we used tended to overlook small regions of genomic alteration and only detected gains and losses spanning large chromosomal segments, whereas manual curation identifies focal, single-gene mutations. The integrated analysis may also overlook genes with significant CNAs because the gene's expression fails to correlate. For example, our previous manual analysis identified highly significant gains of *Myc, Wnt2, Wnt8a, Ezr,* and *Btbd9*, as well as losses of *Arid3a* and *Arhgef16*, among others (3). However, many of these genes did not appear in the integrative analysis, indicating that combined automated and manual curation is the most thorough option. Furthermore, the integrative analysis did not recognize the short, focal amplicon harboring *Wnt2, Met, Cav1*, and *Cav2*. Intriguingly, among the genes that appeared in both the automated analysis and manual curation were *Arid3a* and *Map2k2*, which were among the most commonly occurring genes among the cancer pathways (Figure 2B). With our determination of putative oncogenic events, further experimental studies remain to determine the relative impact of these aberrations.

The gene expression, flow cytometric analysis, and tumorsphere-forming ability of TBP tumor cells indicate an enrichment of stem/progenitor cells among TBP tumors, which may contribute to their aggressive tumorigenicity. Perturbed embryonic signaling pathways like the Wnt pathway may provide a common thread underlying the intrinsic molecular subtype breast cancer signatures, stem/progenitor tumor phenotypes, and EMT induction. Although more commonly associated with colon cancer, recent reports link Wnt activity to EMT (46), the acquisition of stem cell properties (47), and pulmonary metastasis (48) in breast cancer. Targeting these and other morphogenetic signaling pathways may offer more effective treatments for TNBC compared to the current cytotoxic therapies, which are the mainline treatments for TNBC. By sensitizing tumor-initiating cells, morphogen suppression could potentially broaden the therapeutic window and thereby spare normal stem cells from treatment-associated toxicities. Our therapeutic inhibition of *Wnt*, however, is just one example of a variety of potential cancer drivers identified in this study that should be targeted in future experiments. The novel TBP mouse model may therefore be especially well-suited for the preclinical evaluation of better therapy regimens for the most aggressive forms of TNBC.

Acknowledgements

This work was supported by funding from grant ACS IRG-93-033-15, the Simeon J. Fortin Charitable Foundation, and the Pink Revolution Breast Cancer Alliance to KS.

We thank Dr. Leslie Ann Smullin Bourne, Dr. Mark Olof Johnson, Mr. Isaac Nathan Smullin Johnson, Mr. Samuel Smullin, Dr. Robert Smullin, Mr. Dempsey, and Mr. Hohn for their generous support and the members of the Simin lab for their technical assistance.

References

1 Siegel R, Desantis C, Virgo K, Stein K, Mariotto A, Smith T, Cooper D, Gansler T, Lerro C, Fedewa S, Lin C, Leach C, Cannady RS, Cho H, Scoppa S, Hachey M, Kirch R, Jemal A and Ward E: Cancer treatment and survivorship statistics, 2012. CA Cancer J Clin *62(4)*: 220-241, 2012.

2 Eifert C and Powers RS: From cancer genomes to oncogenic drivers, tumour dependencies and therapeutic targets. Nat Rev Cancer *12*: 572-578, 2012.

3 Kumar P, Mukherjee M, Johnson JP, Patel M, Huey B, Albertson DG and Simin K: Cooperativity of Rb, Brca1, and p53 in malignant breast cancer evolution. PLoS Genet *8(11)*: e1003027, 2012.

4 Carey L, Winer E, Viale G, Cameron D and Gianni L: Triple-negative breast cancer: Disease entity or title of convenience? Nat Rev Clin Oncol *7(12)*: 683-692, 2010.

5 Herschkowitz JI, Simin K, Weigman VJ, Mikaelian I, Usary J, Hu Z, Rasmussen KE, Jones LP, Assefnia S, Chandrasekharan S, Backlund MG, Yin Y, Khramtsov AI, Bastein R, Quackenbush J, Glazer RI, Brown PH, Green JE, Kopelovich L, Furth PA, Palazzo JP, Olopade OI, Bernard PS, Churchill GA, Van Dyke T and Perou CM: Identification of conserved gene expression features between murine mammary carcinoma models and human breast tumors. Genome Biol *8(5)*: R76, 2007.

6 Venkatraman ES and Olshen AB: A faster circular binary segmentation algorithm for the analysis of array CGH data. Bioinformatics *23(6)*: 657-663, 2007.

7 Beroukhim R, Getz G, Nghiemphu L, Barretina J, Hsueh T, Linhart D, Vivanco I, Lee JC, Huang JH, Alexander S, Du J, Kau T, Thomas RK, Shah K, Soto H, Perner S, Prensner J, Debiasi RM, Demichelis F, Hatton C, Rubin MA, Garraway LA, Nelson SF, Liau L, Mischel PS, Cloughesy TF, Meyerson M, Golub TA, Lander ES, Mellinghoff IK and Sellers WR: Assessing the significance of chromosomal aberrations in cancer: Methodology and application to glioma. Proc Natl Acad Sci USA *104(50)*: 20007-20012, 2007.

8 Kenny PA, Enver T and Ashworth A: Receptor and secreted targets of Wnt-1/beta-catenin signalling in mouse mammary epithelial cells. BMC Cancer *5*: 3, 2005.

9 Shackleton M, Vaillant F, Simpson KJ, Stingl J, Smyth GK, Asselin-Labat ML, Wu L, Lindeman GJ and Visvader JE: Generation of a functional mammary gland from a single stem cell. Nature *439(7072)*: 84-88, 2006.

10 Stingl J, Eirew P, Ricketson I, Shackleton M, Vaillant F, Choi D, Li HI and Eaves CJ: Purification and unique properties of mammary epithelial stem cells. Nature *439(7079)*: 993-997, 2006.

11 Dontu G, Al-Hajj M, Abdallah WM, Clarke MF and Wicha MS: Stem cells in normal breast development and breast cancer. Cell Prolif *36(Suppl 1)*: 59-72, 2003.

12 Staebler A, Heselmeyer-Haddad K, Bell K, Riopel M, Perlman E, Ried T and Kurman RJ: Micropapillary serous carcinoma of the ovary has distinct patterns of chromosomal imbalances by comparative genomic hybridization compared with atypical proliferative serous tumors and serous carcinomas. Hum Pathol *33(1)*: 47-59, 2002.

13 Zhou J, Roh JW, Bandyopadhyay S, Chen Z, Munkarah A, Hussein Y, Alosh B, Jazaerly T, Hayek K, Sood AK and Ali-Fehmi R: Overexpression of enhancer of zeste homolog 2 (EZH2) and focal adhesion kinase (FAK) in high grade endometrial carcinoma. Gynecol Oncol, 2012.

14 Cheng YX, Qi XY, Huang JL, Hu M, Zhou LM, Li BS and Xu XX: Toll-like receptor 4 signaling promotes the immunosuppressive cytokine production of human cervical cancer. Eur J Gynaecol Oncol *33(3)*: 291-294, 2012.

15 Zhang Y, Wang Y, Yuan J, Qin W, Liu F, Wang F, Zhang G and Yang X: Toll-like receptor 4 ligation confers chemoresistance to docetaxel on PC-3 human prostate cancer cells. Cell Biol Toxicol *28(4)*: 269-277, 2012.

16 Cano KE, Li L, Bhatia S, Bhatia R, Forman SJ and Chen Y: NMR-based metabolomic analysis of the molecular pathogenesis of therapy-related myelodysplasia/acute myeloid leukemia. J Proteome Res *10(6)*: 2873-2881, 2011.

17 Creighton C, Hanash S and Beer D: Gene expression patterns define pathways correlated with loss of differentiation in lung adenocarcinomas. FEBS Lett *540(1-3)*: 167-170, 2003.

18 Candi E, Schmidt R and Melino G: The cornified envelope: A model of cell death in the skin. Nat Rev Mol Cell Biol *6(4)*: 328-340, 2005.

19 Shah SP, Roth A, Goya R, Oloumi A, Ha G, Zhao Y, Turashvili G, Ding J, Tse K, Haffari G, Bashashati A, Prentice LM, Khattra J, Burleigh A, Yap D, Bernard V, McPherson A, Shumansky K, Crisan A, Giuliany R, Heravi-Moussavi A, Rosner J, Lai D, Birol I, Varhol R, Tam A, Dhalla N, Zeng T, Ma K, Chan SK, Griffith M, Moradian A, Cheng SW, Morin GB, Watson P, Gelmon K, Chia S, Chin SF, Curtis C, Rueda OM, Pharoah PD, Damaraju S, Mackey J, Hoon K, Harkins T, Tadigotla V, Sigaroudinia M, Gascard P, Tlsty T, Costello JF, Meyer IM, Eaves CJ, Wasserman WW, Jones S, Huntsman D, Hirst M, Caldas C, Marra MA and Aparicio S: The clonal and mutational evolution spectrum of primary triple-negative breast cancers. Nature *486(7403)*: 395-399, 2012.

20 Ellis MJ, Ding L, Shen D, Luo J, Suman VJ, Wallis JW, Van Tine BA, Hoog J, Goiffon RJ, Goldstein TC, Ng S, Lin L, Crowder R, Snider J, Ballman K, Weber J, Chen K, Koboldt DC, Kandoth C, Schierding WS, McMichael JF, Miller CA, Lu C, Harris CC, McLellan MD, Wendl MC, DeSchryver K, Allred DC, Esserman L, Unzeitig G, Margenthaler J, Babiera GV, Marcom PK, Guenther JM, Leitch M, Hunt K, Olson J, Tao Y, Maher CA, Fulton LL, Fulton RS, Harrison M, Oberkfell B, Du F, Demeter R, Vickery TL, Elhammali A, Piwnica-Worms H, McDonald S, Watson M, Dooling DJ, Ota D, Chang LW, Bose R, Ley TJ, Piwnica-Worms D, Stuart JM, Wilson RK and Mardis ER: Whole-genome analysis informs breast cancer response to aromatase inhibition. Nature *486(7403)*: 353-360, 2012.

21 Krystof V and Uldrijan S: Cyclin-dependent kinase inhibitors as anticancer drugs. Curr Drug Targets *11(3)*: 291-302, 2010.

22 Fonseca SG, Gromada J and Urano F. Endoplasmic reticulum stress and pancreatic beta-cell death. Trends Endocrinol Metab *22(7)*: 266-274, 2011.

23 Kadowaki H, Nishitoh H, Urano F, Sadamitsu C, Matsuzawa A, Takeda K, Masutani H, Yodoi J, Urano Y, Nagano T and Ichijo H: Amyloid beta induces neuronal cell death through ROS-mediated ASK1 activation. Cell Death Differ *12(1)*: 19-24, 2005.

24 Stefani IC, Wright D, Polizzi KM and Kontoravdi C: The role of ER stress-induced apoptosis in neurodegeneration. Curr Alzheimer Res *9(3)*: 373-387, 2012.

25 Takebe N, Warren RQ and Ivy SP: Breast cancer growth and metastasis: Interplay between cancer stem cells, embryonic signaling pathways and epithelial-to-mesenchymal transition. Breast Cancer Res *13(3)*: 211, 2011.

26 Li Y, Welm B, Podsypanina K, Huang S, Chamorro M, Zhang X, Rowlands T, Egeblad M, Cowin P, Werb Z, Tan LK, Rosen JM and Varmus HE: Evidence that transgenes encoding components of the Wnt signaling pathway preferentially induce mammary cancers from progenitor cells. Proc Natl Acad Sci USA *100(26)*: 15853-15858, 2003.

27 Lim E, Vaillant F, Wu D, Forrest NC, Pal B, Hart AH, Asselin-Labat ML, Gyorki DE, Ward T, Partanen A, Feleppa F, Huschtscha LI, Thorne HJ, kConFab, Fox SB, Yan M, French JD, Brown MA, Smyth GK, Visvader JE and Lindeman GJ: Aberrant luminal progenitors as the candidate target population for basal tumor development in BRCA1 mutation carriers. Nat Med *15(8)*: 907-913, 2009.

28 Hennessy BT, Gonzalez-Angulo AM, Stemke-Hale K, Gilcrease MZ, Krishnamurthy S, Lee JS, Fridlyand J, Sahin A, Agarwal R, Joy C, Liu W, Stivers D, Baggerly K, Carey M, Lluch A, Monteagudo C, He X, Weigman V, Fan C, Palazzo J, Hortobagyi GN, Nolden LK, Wang NJ, Valero V, Gray JW, Perou CM and Mills GB: Characterization of a naturally occurring breast cancer subset enriched in epithelial-to-mesenchymal transition and stem cell characteristics. Cancer Res *69(10)*: 4116-4124, 2009.

29 Prat A, Parker JS, Karginova O, Fan C, Livasy C, Herschkowitz JI, He X and Perou CM: Phenotypic and molecular characterization of the claudin-low intrinsic subtype of breast cancer. Breast Cancer Res *12(5)*: R68, 2010.

30 Shackleton M, Vaillant F, Simpson KJ, Stingl J, Smyth GK, Asselin-Labat ML, Wu L, Lindeman GJ and Visvader JE: Generation of a functional mammary gland from a single stem cell. Nature *439(7072)*: 84-88, 2006.

31 Stingl J, Eirew P, Ricketson I, Shackleton M, Vaillant F, Choi D, Li HI and Eaves CJ: Purification and unique properties of mammary epithelial stem cells. Nature *439(7079)*: 993-997, 2006.

32 Liu JC, Deng T, Lehal RS, Kim J and Zacksenhaus E: Identification of tumorsphere- and tumor-initiating cells in HER2/Neu-induced mammary tumors. Cancer Res *67(18)*: 8671-8681, 2007.

33 Cho RW, Wang X, Diehn M, Shedden K, Chen GY, Sherlock G, Gurney A, Lewicki J and Clarke MF: Isolation and molecular characterization of cancer stem cells in MMTV-wnt-1 murine breast tumors. Stem Cells *26(2)*: 364-371, 2008.

34 Vaillant F, Asselin-Labat ML, Shackleton M, Forrest NC, Lindeman GJ and Visvader JE: The mammary progenitor marker CD61/beta3 integrin identifies cancer stem cells in mouse models of mammary tumorigenesis. Cancer Res *68(19)*: 7711-7717, 2008.

35 Dontu G, Al-Hajj M, Abdallah WM, Clarke MF and Wicha MS: Stem cells in normal breast development and breast cancer. Cell Prolif *36(Suppl 1)*: 59-72, 2003.

36 Ponti D, Costa A, Zaffaroni N, Pratesi G, Petrangolini G, Coradini D, Pilotti S, Pierotti MA and Daidone MG: Isolation and *in vitro* propagation of tumorigenic breast cancer cells with stem/progenitor cell properties. Cancer Res *65(13)*: 5506-5511, 2005.

37 Huang SM, Mishina YM, Liu S, Cheung A, Stegmeier F, Michaud GA, Charlat O, Wiellette E, Zhang Y, Wiessner S, Hild M, Shi X, Wilson CJ, Mickanin C, Myer V, Fazal A, Tomlinson R, Serluca F, Shao W, Cheng H, Shultz M, Rau C, Schirle M, Schlegl J, Ghidelli S, Fawell S, Lu C, Curtis D, Kirschner MW, Lengauer C, Finan PM, Tallarico JA, Bouwmeester T, Porter JA, Bauer A and Cong F: Tankyrase inhibition stabilizes axin and antagonizes wnt signalling. Nature *461(7264)*: 614-620, 2009.

38 Simin K, Wu H, Lu L, Pinkel D, Albertson D, Cardiff RD and Van Dyke T: pRb inactivation in mammary cells reveals common mechanisms for tumor initiation and progression in divergent epithelia. PLoS Biol *2(2)*: E22, 2004.

39 Jiang Z, Deng T, Jones R, Li H, Herschkowitz JI, Liu JC, Weigman VJ, Tsao MS, Lane TF, Perou CM and Zacksenhaus E: Rb deletion in mouse mammary progenitors induces luminal-B or basal-like/EMT tumor subtypes depending on p53 status. J Clin Invest *120(9)*: 3296-3309, 2010.

40 Da Silva L, Simpson PT, Smart CE, Cocciardi S, Waddell N, Lane A, Morrison BJ, Vargas AC, Healey S, Beesley J, Pakkiri P, Parry S, Kurniawan N, Reid L, Keith P, Faria P, Pereira E, Skalova A, Bilous M, Balleine RL, Do H, Dobrovic A, Fox S, Franco M, Reynolds B, Khanna KK, Cummings M, Chenevix-Trench G and Lakhani SR: HER3 and downstream pathways are involved in colonization of brain metastases from breast cancer. Breast Cancer Res *12(4)*: R46, 2010.

41 Albertson DG: Profiling breast cancer by array CGH. Breast Cancer Res Treat *78(3)*: 289-298, 2003.

42 Holstege H, van Beers E, Velds A, Liu X, Joosse SA, Klarenbeek S, Schut E, Kerkhoven R, Klijn CN, Wessels LF, Nederlof PM and Jonkers J: Cross-species comparison of aCGH data from mouse and human *BRCA1*- and *BRCA2*-mutated breast cancers. BMC Cancer *10*: 455, 2010.

43 Solvang HK, Lingjaerde OC, Frigessi A, Borresen-Dale AL and Kristensen VN: Linear and non-linear dependencies between copy number aberrations and mRNA expression reveal distinct molecular pathways in breast cancer. BMC Bioinformatics *12*: 197, 2011.

44 Xu K, Usary J, Kousis PC, Prat A, Wang DY, Adams JR, Wang W, Loch AJ, Deng T, Zhao W, Cardiff RD, Yoon K, Gaiano N, Ling V, Beyene J, Zacksenhaus E, Gridley T, Leong WL, Guidos CJ, Perou CM and Egan SE: Lunatic fringe deficiency cooperates with the Met/Caveolin gene amplicon to induce basal-like breast cancer. Cancer Cell *21(5)*: 626-641, 2012.

45 Gastaldi S, Sassi F, Accornero P, Torti D, Galimi F, Migliardi G, Molyneux G, Perera T, Comoglio PM, Boccaccio C, Smalley MJ, Bertotti A and Trusolino L: Met signaling regulates growth, repopulating potential and basal cell-fate commitment of mammary luminal progenitors: Implications for basal-like breast cancer. Oncogene *32(11)*: 1428-1440, 2013.

46 Scheel C, Eaton EN, Li SH, Chaffer CL, Reinhardt F, Kah KJ, Bell G, Guo W, Rubin J, Richardson AL and Weinberg RA: Paracrine and autocrine signals induce and maintain mesenchymal and stem cell states in the breast. Cell *145(6)*: 926-940, 2011.

47 Mani SA, Guo W, Liao MJ, Eaton EN, Ayyanan A, Zhou AY, Brooks M, Reinhard F, Zhang CC, Shipitsin M, Campbell LL, Polyak K, Brisken C, Yang J and Weinberg RA: The epithelial-mesenchymal transition generates cells with properties of stem cells. Cell *133(4)*: 704-715, 2008.

48 DiMeo TA, Anderson K, Phadke P, Fan C, Perou CM, Naber S and Kuperwasser C: A novel lung metastasis signature links wnt signaling with cancer cell self-renewal and epithelial-mesenchymal transition in basal-like breast cancer. Cancer Res *69(13)*: 5364-5373, 2009.

Received January 17, 2014
Revised March 21, 2014
Accepted March 24, 2014